STEM CELLS TRANSLATIONAL MEDICINE℠

TISSUE ENGINEERING AND REGENERATIVE MEDICINE

Bioengineered Myocardium Derived from Induced Pluripotent Stem Cells Improves Cardiac Function and Attenuates Cardiac Remodeling Following Chronic Myocardial Infarction in Rats

KENJI MIKI,[a] HISAZUMI UENAKA,[a] ATSUHIRO SAITO,[b] SHIGERU MIYAGAWA,[a] TAICHI SAKAGUCHI,[a] TAKAHIRO HIGUCHI,[a] TATSUYA SHIMIZU,[c] TERUO OKANO,[c] SHINYA YAMANAKA,[d,e,f,g] YOSHIKI SAWA[a,b]

Key Words. Induced pluripotent stem cells • Bioengineered myocardium • Implantation • Myocardial infarction

[a]Department of Surgery, Division of Cardiovascular Surgery, Osaka University Graduate School of Medicine, Osaka, Japan; [b]Medical Center for Translational Research, Osaka University Hospital, Osaka, Japan; [c]Institute of Advanced Biomedical Engineering and Science, Tokyo Women's Medical University, Tokyo, Japan; [d]Center for iPS Cell Research and Application (CiRA) and [e]Institute for Integrated Cell-Material Sciences, Kyoto University, Kyoto, Japan; [f]Yamanaka iPS Cell Special Project, Japan Science and Technology Agency, Kawaguchi, Japan; [g]Gladstone Institute of Cardiovascular Disease, San Francisco, California, USA

Correspondence: Yoshiki Sawa, M.D., Ph.D., Department of Surgery, Division of Cardiovascular Surgery, Osaka University Graduate School of Medicine, 2-2-E1 Yamada-oka, Suita, Osaka 565-0871, Japan. Telephone: 81-6-6879-3154; Fax: 81-6-6879-3163; e-mail: sawa-p@tissue.med.osaka-u.ac.jp

Received October 12, 2011; accepted for publication April 13, 2012; first published online in SCTM *EXPRESS* May 14, 2012.

1066-5099/2012/$20.00/0

http://dx.doi.org/10.5966/sctm.2011-0038

ABSTRACT

Cell-based therapies are promising strategies for myocardial repair following myocardial infarction. Induced pluripotent stem (iPS) cells have the potential to generate many cardiomyocytes, and they hold significant promise for the application of regenerative medicine to heart failure. Here, we developed cardiac tissue sheets, termed bioengineered myocardium (BM), from mouse iPS cells and measured cardiac performance following BM implantation in a rat chronic myocardial infarction model. Immunostaining analyses revealed that the α-actinin$^+$ cell population was isolated with more than 99% purity under specific culture conditions. To evaluate the contribution of BM to the improvements in cardiac performance, we induced myocardial infarction in 30 F344/NJcl-*rnu*/*rnu* rats by left anterior descending coronary ligation. The rats were randomly divided into two groups, 2 weeks after ligation: a BM implantation group ($n = 15$) and a sham group ($n = 15$). Echocardiography and catheter examination showed that the BM implantation significantly improved cardiac function and attenuated cardiac remodeling compared with the sham group. Histological analyses demonstrated that the implanted BM survived at the epicardial implantation site 4 weeks after implantation. The implanted BM survived and attenuated left ventricular remodeling in the rat chronic myocardial infarction model. Thus, BM derived from iPS cells might be a promising new treatment for heart failure. STEM CELLS TRANSLATIONAL MEDICINE *2012;1:430–437*

INTRODUCTION

Even though remarkable progress has been made in the medical and surgical management of cardiac diseases, heart failure remains a major cause of death worldwide [1, 2]. Cell-based therapies using skeletal myoblasts, bone marrow mononuclear cells, mesenchymal stem cells, and cardiac stem cells were recently introduced for the clinical treatment of ischemic heart disease [3–6]. Bolli et al. [6] reported that intracoronary infusion of autologous cardiac stem cells is effective in improving left ventricular (LV) systolic function and reducing infarct size in patients with heart failure after myocardial infarction (MI). However, other studies [3–5] showed that their effectiveness is limited and that long-term outcomes are unfavorable.

Growth factors secreted from the transplanted cells are thought to improve the damaged myocardium to a certain extent; this occurs via a paracrine effect [7, 8]. Myoblasts or bone marrow mononuclear cells may improve cardiac performance via a paracrine effect, without directly contributing to the improvement of systolic performance by enhancing the contractile ability of the heart [9, 10]. Several researchers have developed certain stem or progenitor cells that can differentiate into cardiomyocytes or generate cardiomyocytes via cell fusion [11, 12], in order to obtain cells that can compensate for lost cardiomyocytes and greatly promote myocardial regeneration in a severely damaged myocardium following transplantation [13, 14]. However, the differentiation rate of these stem or progenitor cells into cardiomyocytes, or their fusion rate, is relatively low. Therefore, improvement of the impaired cardiac performance by these cells is probably mainly due to paracrine effects.

We think that two important issues need to be addressed in order to improve the effectiveness of cell-based therapies for heart failure. First, autologous stem cells, which differentiate into definitive cardiomyocytes at high rates, need to be used to greatly enhance the contractile ability of the myocardium in situations where

large numbers of cardiomyocytes are damaged. Second, these cells need to be delivered to the damaged myocardium at the maximum dose by using sophisticated cell delivery systems. For example, the development of systems that will enable newly generated cardiomyocytes to integrate with each other ex vivo to form cardiac tissue, and enable this cardiac tissue to synchronously contract with the host myocardium following implantation, should be investigated. Such a strategy may provide the best method for regenerating a severely damaged myocardium.

An intelligent cell delivery system, termed cell sheet technology, was recently developed [15–17]. Conventional methods of cell delivery present some disadvantages, such as needle injection, loss of transplanted cells by leakage, poor survival of grafted cells, myocardial damage resulting from injury by the needle and subsequent acute inflammation [18, 19], and the potential to cause a lethal arrhythmia [20]. However, a cell sheet can deliver substantially higher cell numbers to the damaged myocardium than can needle injection, and it can induce significant myocardial regeneration [21]. Pluripotent stem cells have been generated from mouse and human somatic cells by using specific transcription factors (OCT4, SOX2, c-MYC, and KLF4 or OCT4, SOX2, NANOG, and LIN28) [22–24]; cell-based therapy using such induced pluripotent stem (iPS) cells is expected to find widespread clinical applications. There have been several reports on the differentiation of iPS cells into cardiomyocytes [25–27], but it is unknown whether cardiac tissue sheets derived from iPS cells can improve cardiac function in a chronic MI model. In this study, we developed cardiac tissue sheets termed bioengineered myocardium (BM) from mouse iPS cells, and investigated the efficacy of BM derived from iPS cells in a chronic MI model.

Materials and Methods

Cardiac Differentiation of iPS Cells and Purification of iPS Cell-Derived Cardiomyocytes

We cultured and maintained mouse iPS cells (256H18) [28] and embryonic stem (ES) cells (B6G2) on feeder layers of mitomycin-C-treated STO cells (supplemental online data) [22]. For differentiation, 500 iPS cells were resuspended in 30-μl aliquots of differentiation medium (DM; growth medium without leukemia inhibitory factor) and cultured in 96-well HydroCell plates (CellSeed, Tokyo, http://www.cellseed.com) for 2 days. On day 2, an additional 30 μl of DM containing 4 μM 6-bromoindirubin-3′-oxime (BIO; a glycogen synthase kinase-3β inhibitor, to activate the Wnt-signaling pathway) (Calbiochem, San Diego, http://www.emdbiosciences.com) [29] was added to each well. On day 5, the individual embryoid bodies (EBs) obtained were transferred to gelatin-coated 60-mm dishes (200 EBs per dish). The medium was replenished with fresh DM every day. On day 11, the medium was changed to no-glucose Dulbecco's modified Eagle's medium (DMEM) (Invitrogen, Carlsbad, CA, http://www.invitrogen.com) (F. Hattori and K. Fukuda, WO2007/088874; PCT/JP2007/051563, 2007), and the cells were maintained for a further 2–3 days. The medium was then replaced with DM, and on day 15, the cells were used for reverse transcription-polymerase chain reaction (RT-PCR), quantitative RT-PCR, or immunocytochemistry (supplemental online data).

Development of the iPS Cell-Derived Contractile BM

To develop the contracting BM from iPS cells, individual EBs were seeded onto 24-well UpCell plates (CellSeed) (40 EBs per well) on day 5. Each UpCell plate contains cell culture surfaces to which a temperature-responsive polymer, poly(*N*-isopropylacrylamide), is grafted, and from which cells can be detached as a cell sheet simply by reducing the temperature without any enzymatic treatments [15–17].

Next, the medium was changed to DM and no-glucose DMEM as outlined above, until day 15. The iPS cell-derived cardiomyocytes were then detached at room temperature as a cell sheet with a diameter of approximately 10 mm (supplemental online Fig. 1). This cardiac tissue sheet, termed BM, exhibited spontaneous contraction (supplemental online Movie 1) and was used for implantation.

Animal Experiments

We used F344/NJcl-*rnu/rnu* female rats (CLEA Japan, Tokyo, http://www.clea-japan.com) in which MI was induced by left anterior descending (LAD) coronary ligation [21, 30, 31]. Two weeks later, the animals were randomly divided into two groups: the BM implantation group ($n = 15$) and the sham group ($n = 15$) in which we carried out MI surgery, and opened and closed the rat chests 2 weeks later. BM was implanted directly over the scar area without sutures. After detachment from the temperature-responsive dish, the BM was picked up and spread over the surface of the heart, following which it was allowed to attach to the host myocardium for 10–15 minutes. The animal experiments were performed in compliance with the Principles of Laboratory Animal Care formulated by the National Society for Medical Research, and the Guide for the Care and Use of Laboratory Animals prepared by the Institute of Laboratory Animal Resource and published by the National Institutes of Health (NIH Publication No. 86-23, revised 1996). The ethics committee of Osaka University approved all experiments.

Assessment of Cardiac Performance

Echocardiography was performed before implantation and 1, 2, and 4 weeks after implantation. We measured the anterior wall dimension, posterior wall dimension, left ventricular diastolic dimension (LVDd), and left ventricular systolic dimension (LVDs), and then we calculated the LV ejection fraction (EF) and fractional shortening (FS). EF and FS were calculated using the following formulas:

$$\mathrm{EF}\ (\%) = [(\mathrm{LVDd}^3 - \mathrm{LVDs}^3)/\mathrm{LVDd}^3] \times 100$$

$$\mathrm{FS}\ (\%) = [(\mathrm{LVDd} - \mathrm{LVDs})/\mathrm{LVDd}] \times 100$$

A catheter examination was performed 4 weeks after implantation; sternotomy was performed using a thin catheter tip, and hemodynamics parameters such as dP/dt (an index that is used clinically to characterize the contractile ability of the heart) maximum (max), dP/dt minimum (min), the time constant of isovolumic relaxation (τ), end-systolic elastance (Ees), and end-diastolic elastance (Eed) were determined.

Preparation of LV Myocardium Specimens for Histological Analysis and RNA Isolation

After performing echocardiography and catheter examination, the hearts ($n = 15$ per group) were removed 4 weeks following

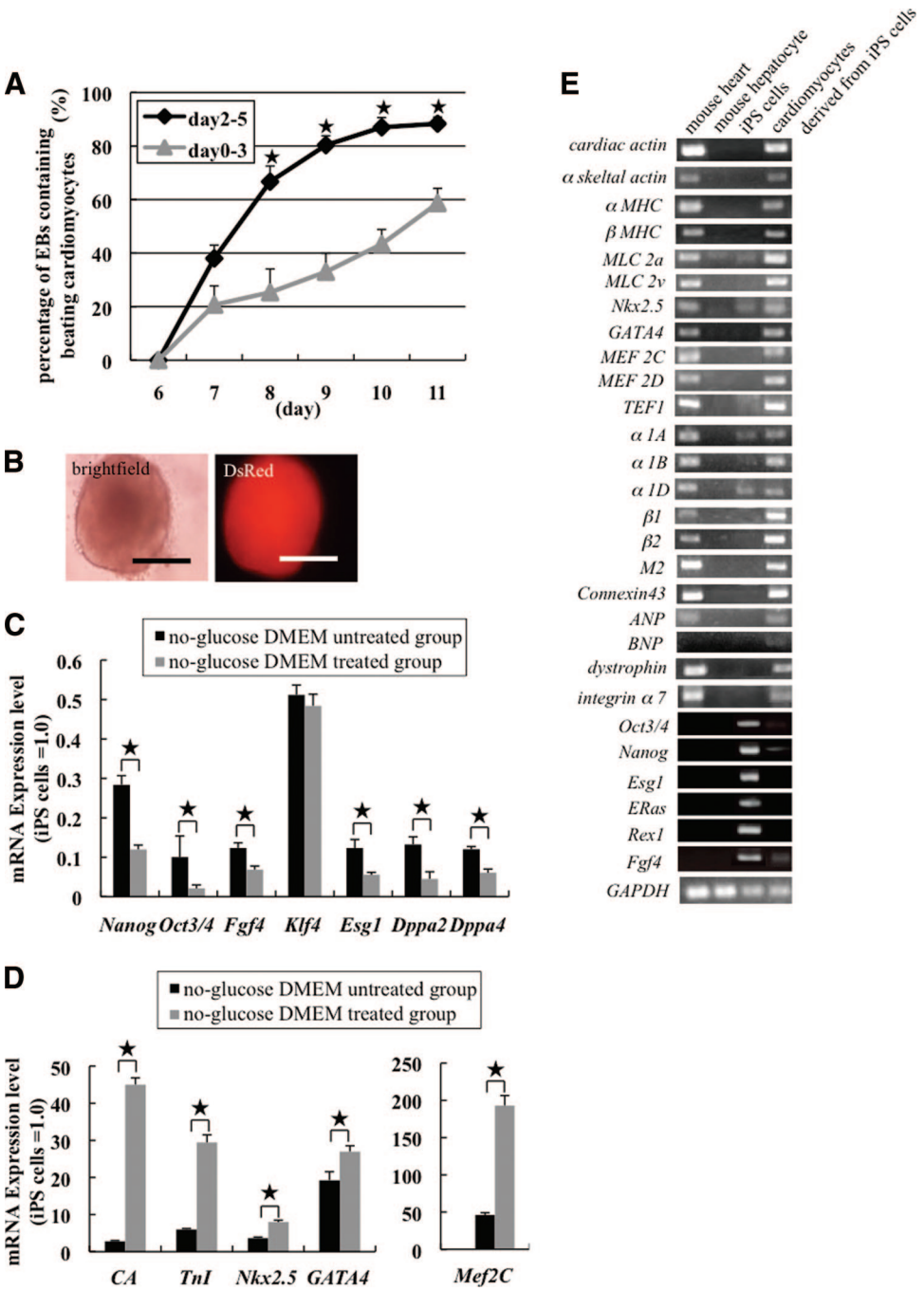

Figure 1. Efficiency of differentiation of mouse iPS cells into cardiomyocytes. **(A):** Number of EBs with beating foci. ⋆, $p < .05$. **(B):** Image of an EB derived from iPS cells obtained on day 5. DsRed was expressed in the EB because the mouse iPS cell line 256H18 was used. Scale bars = 300 μm. **(C–E):** Gene expression in iPS cell-derived cardiomyocytes. Quantitative reverse transcription-polymerase chain reaction (RT-PCR) analyses of the expression levels of undifferentiated cell marker genes (*Nanog*, *Oct3/4*, *Fgf4*, *Esg1*, *Dppa2*, and *Dppa4*) **(C)** and cardiac marker genes (*cardiac actin* [*CA*], *Troponin I* [*TnI*], *Nkx2.5*, *GATA4*, and *Mef2C*) **(D)** in the no-glucose DMEM-treated group and the no-glucose DMEM-untreated group ($n = 5$ per group). ⋆, $p < .05$. **(E):** RT-PCR analyses of cardiac marker genes, such as those for structural proteins (*cardiac actin* to *MLC2v*), transcription factors (*Nkx2.5* to *TEF1*), adrenergic receptors (α*1A* to β*2*), muscarinic receptors (*M2*), other proteins (*connexin 43* to *integrin* α*7*), and markers for undifferentiated cells (*Oct3/4* to *Fgf4*) in native cardiomyocytes, native hepatocytes, iPS cells, and iPS cell-derived cardiomyocytes. Abbreviations: DMEM, Dulbecco's modified Eagle's medium; DsRed, *Discosoma* red fluorescent protein; iPS, induced pluripotent stem.

implantation and sectioned into two pieces each. Each heart was cut into cross-sections for nine specimens in each group, with one section snap-frozen in liquid nitrogen and two others embedded in O.C.T. compound (Sakura Finetek Japan, Tokyo, http://www.sakura-finetek.com) for immunostaining and Masson's trichrome staining. Fibrosis areas were calculated using MetaMorph Microscopy Automation and Image Analysis Software (Molecular Devices Corp., Union City, CA, http://www.moleculardevices.com). The remaining six specimens in each group were transverse-sectioned; the apex-side specimens were

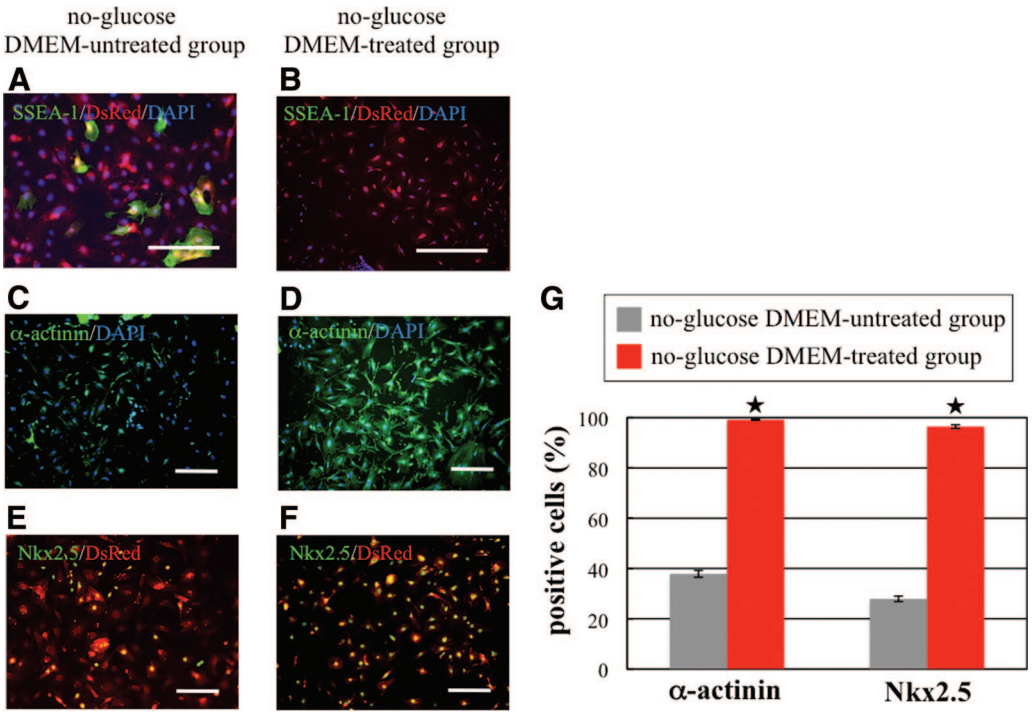

Figure 2. Immunostaining of induced pluripotent stem (iPS) cell-derived cardiomyocytes. **(A–F):** Microscopic images showing differentiated cells on day 15 in the no-glucose DMEM-untreated group **(A, C, E)** and in the no-glucose DMEM-treated group **(B, D, F)**. **(A, B):** Immunostaining of SSEA-1 (green). Nuclei were stained with DAPI (blue); DsRed (red) was expressed in the cytosol of iPS cell-derived cells. Scale bars = 100 μm. **(C, D):** Immunostaining of α-actinin (green). Nuclei were stained with DAPI. Scale bars = 300 μm. **(E, F):** Immunostaining of Nkx2.5 (green) and DsRed (red) expression in the cytosol of iPS cell-derived cells. Scale bars = 300 μm. **(G):** Quantification of α-actinin- and Nkx2.5-positive cells by imaging analysis. In the no-glucose DMEM-untreated group (gray columns), the percentages of α-actinin- and Nkx2.5-positive cells were 37.87% and 27.92%, respectively. In contrast, the percentages of α-actinin- and Nkx2.5-positive cells in the no-glucose DMEM-treated group (red column) were 99.18% and 96.45%, respectively. ⋆, $p < .05$. Abbreviations: DAPI, 4′,6-diamidino-2-phenylindole; DMEM, Dulbecco's modified Eagle's medium; DsRed, *Discosoma* red fluorescent protein; SSEA, stage-specific embryonic antigen.

dissected to remove the right ventricular free wall and divided into two pieces from either the infarction or the remote sites. Each specimen was stored in RNAlater solution (Qiagen, Hilden, Germany, http://www1.qiagen.com) for RNA isolation and in T-PER Tissue Protein Extraction Reagent (Thermo Fisher Scientific, Waltham, MA, http://www.thermofisher.com) for the enzyme-linked immunosorbent assay (ELISA) (supplemental online data).

Statistical Analysis

All values are expressed as mean (SD). Statistical comparison of the data was performed using unpaired two-sided *t* tests. A *p* value of $<.05$ was considered statistically significant.

Results

Expression of Several Cardiac Markers by iPS Cell-Derived Cardiomyocytes and Procurement of α-Actinin-Positive Cardiomyocytes with More than 99% Purity

To obtain high-purity cardiomyocytes from iPS cells (256H18 clone), we first generated EBs by treatment with BIO and determined the best culture conditions to induce the differentiation of iPS cells into cardiomyocytes. When EBs were cultured with BIO from day 2 until day 5, spontaneous contraction occurred within the small foci in approximately 88% of the EBs on day 11. In contrast, when EBs were cultured with BIO from day 0 until day 3, the number of beating foci significantly decreased from day 8 to day 11 when compared with the cells cultured with BIO from day 2 to day 5 (Fig. 1A). The EBs formed from the 256H18 iPS cell line expressed *Discosoma* red fluorescent protein (DsRed) in the cytosol (Fig. 1B). When EBs derived from ES cells were treated with BIO on days 2–5, they exhibited spontaneous contraction equivalent to that of the iPS cells treated with BIO for the same period (supplemental online Movie 2).

In order to avoid teratoma formation after implantation, we changed the DM to no-glucose DMEM for days 11–12 or 13, and then reverted to DM the next day. This method enabled us to easily select differentiated cardiomyocytes from undifferentiated cells based on their different energy consumption requirements.

We performed RT-PCR, quantitative RT-PCR, and immunostaining with differentiated cells from day 15 to investigate the purification efficiency. Quantitative RT-PCR analysis revealed that the expression of undifferentiated cell marker genes (*Nanog*, *Oct3/4*, *Fgf4*, *Esg1*, *Dppa2*, and *Dppa4*) was significantly lower in the no-glucose DMEM-treated group than in the no-glucose DMEM-untreated group. These data indicated that iPS cells cultured in no-glucose DMEM had lower potential to form tumors following implantation (Fig. 1C). The expression of cardiac marker genes (*cardiac actin*, *TnI*, *Nkx2.5*, *Gata4*, and *Mef2C*) was significantly higher in the no-glucose DMEM-treated group than in the no-glucose DMEM-untreated group (Fig. 1D). Therefore, we surmised that no-glucose DMEM treatment significantly increases the purity of differentiated iPS cell-derived cardiomyocytes by destroying noncardiomyocytes. RT-PCR analysis further revealed that iPS cell-derived cardiomyocytes treated with BIO and no-glucose DMEM expressed several cardiac markers,

such as structural proteins, transcription factors, adrenergic and muscarinic receptors, and connexin 43, to nearly the same extent as the native cardiomyocytes did (Fig. 1E). Conversely, markers (*Oct3/4*, *Nanog*, *Esg1*, *Eras*, *Rex1*, and *Fgf4*) for undifferentiated cells were downregulated in iPS cell-derived cardiomyocytes compared with iPS cells (Fig. 1E). Immunostaining of stage-specific embryonic antigen-1 (SSEA-1) (a marker of undifferentiated cells) revealed that a few SSEA-1-positive cells remained alive in the no-glucose DMEM-untreated group even at day 15, but that SSEA-1-positive cells were observed in the no-glucose DMEM-treated group (Fig. 2A, 2B). In contrast, immunostaining of α-actinin and Nkx2.5 (cardiac markers) revealed that the percentages of α-actinin and Nkx2.5-positive cells in the no-glucose DMEM-untreated group were 37.87% and 27.92%, respectively, but those in the no-glucose DMEM-treated group were 99.18% and 96.45%, respectively (Fig. 2C–2G). Thus, we successfully obtained high-purity cardiomyocytes from iPS cells by using the combined BIO and no-glucose DMEM culture methods.

Improvement in Cardiac Performance and Attenuation of Remodeling by the BM Derived from iPS Cells

We next investigated the therapeutic effect of the BM derived from iPS cells in vivo by inducing MI in F344/NJcl-*rnu/rnu* rats (nude rats) and then implanting the BM derived from iPS cells onto the infarcted area 2 weeks after the infarction. Echocardiographic analysis revealed that FS improved and LVDd decreased in the group implanted with the BM derived from iPS cells (i.e., the BM group) 4 weeks following implantation (Fig. 3A, 3B; supplemental online Table 1). Thus, the BM improved systolic performance and attenuated LV dilatation. The systolic and diastolic performances also improved after implantation, as revealed by pressure-volume analysis (Fig. 3C). The hemodynamics indices were then determined by performing a catheter examination. Significantly higher Ees and lower Eed, higher dP/dt max and lower dP/dt min, and lower τ were observed in the BM group compared with the sham group 4 weeks after implantation (Fig. 4A, 4B). Thus, these parameters indicate that the BM derived from iPS cells improved systolic and diastolic performances.

Survival and Attenuation of Fibrosis by the BM Derived from iPS Cells at the Epicardial Implantation Site 4 Weeks After Implantation

We obtained LV myocardial specimens 4 weeks after implantation to confirm the survival of the implanted BM derived from iPS cells. Masson's trichrome staining revealed less fibrosis and increased thickness of the anterior wall at the site where the BM was implanted (Fig. 5A, 5B, 5E, 5F). Fluorescence microscopy revealed that the implanted BM, which expressed DsRed in the cytosol, survived at the epicardial implantation site (Fig. 5C, 5D, 5G, 5H). Immunohistochemistry revealed that DsRed-positive surviving cells expressed α-actinin in the sarcomere (Fig. 5I–5N). In addition, the percentage of fibrosis in the BM group was significantly lower than that in the sham group (supplemental online Fig. 2). Furthermore, ELISAs performed for hepatocyte growth factor (HGF) and vascular endothelial growth factor (VEGF) revealed that the expression levels of these angiogenic proteins were higher in the BM group than in the sham group (supplemental online Fig. 3). These data indicated that the BM derived from iPS cells also induced a paracrine or autocrine effect by secreting angiogenic factors and inducing angiogenesis in the impaired myocardium. Thus, these data indicate that the BM derived from iPS cells may improve cardiac performance in severely damaged myocardium by directly affecting contractile function and inducing a paracrine effect on angiogenic proteins.

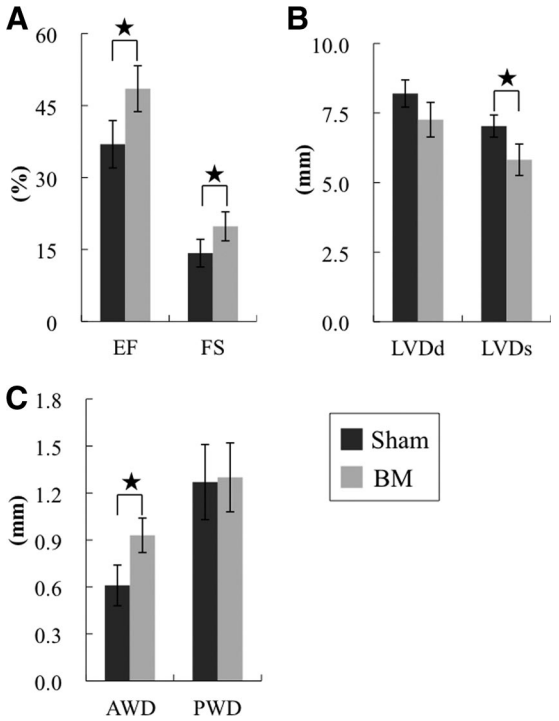

Figure 3. Effects of the induced pluripotent stem cell-derived BM on postinfarct ventricular function at 4 weeks by echocardiography. Shown is echocardiographic assessment of EF **(A)** (left) and FS **(A)** (right), LVDd **(B)** (left), LVDs **(B)** (right), AWD **(C)** (left), and PWD **(C)** (right) in the BM group ($n = 15$) and the sham group ($n = 15$). ⋆, $p < .05$. The systolic performance was significantly improved and the left ventricular dilatation was attenuated in the BM group compared with the sham group. Abbreviations: AWD, anterior wall dimension; BM, bioengineered myocardium; EF, ejection fraction; FS, fractional shortening; LVDd, left ventricular diastolic dimension; LVDs, left ventricular systolic dimension; PWD, posterior wall dimension.

Discussion

We previously demonstrated that neonatal cardiomyocyte sheets can survive in the hearts of rats with chronic MI and that cardiac performance was improved by the successful electrical and histological integration of these sheets into the host myocardium [30]. However, this strategy cannot be used in clinical settings because the large numbers of neonatal cardiomyocytes required cannot be obtained under ethical guidelines. Therefore, we attempted to use autologous iPS cells, due to their high cardiomyocyte differentiation rates. Such cells may completely regenerate a damaged myocardium and contribute to the armamentarium of heart failure management in clinical settings.

Our data indicate that the iPS cell-derived cardiomyocytes, differentiated by combined treatment with BIO and no-glucose DMEM, expressed cardiac markers and were highly similar to native mouse cardiomyocytes. As seen in supplemental online Figure 4, the organization of α-actinin in iPS cell-derived cardiomyocytes was random and similar to that of mouse neonatal cardiomyocytes. We postulate that the iPS cell-derived cardiomyocytes generated using our protocol included embryonic- and adult-phenotype ventricular and atrial myocytes.

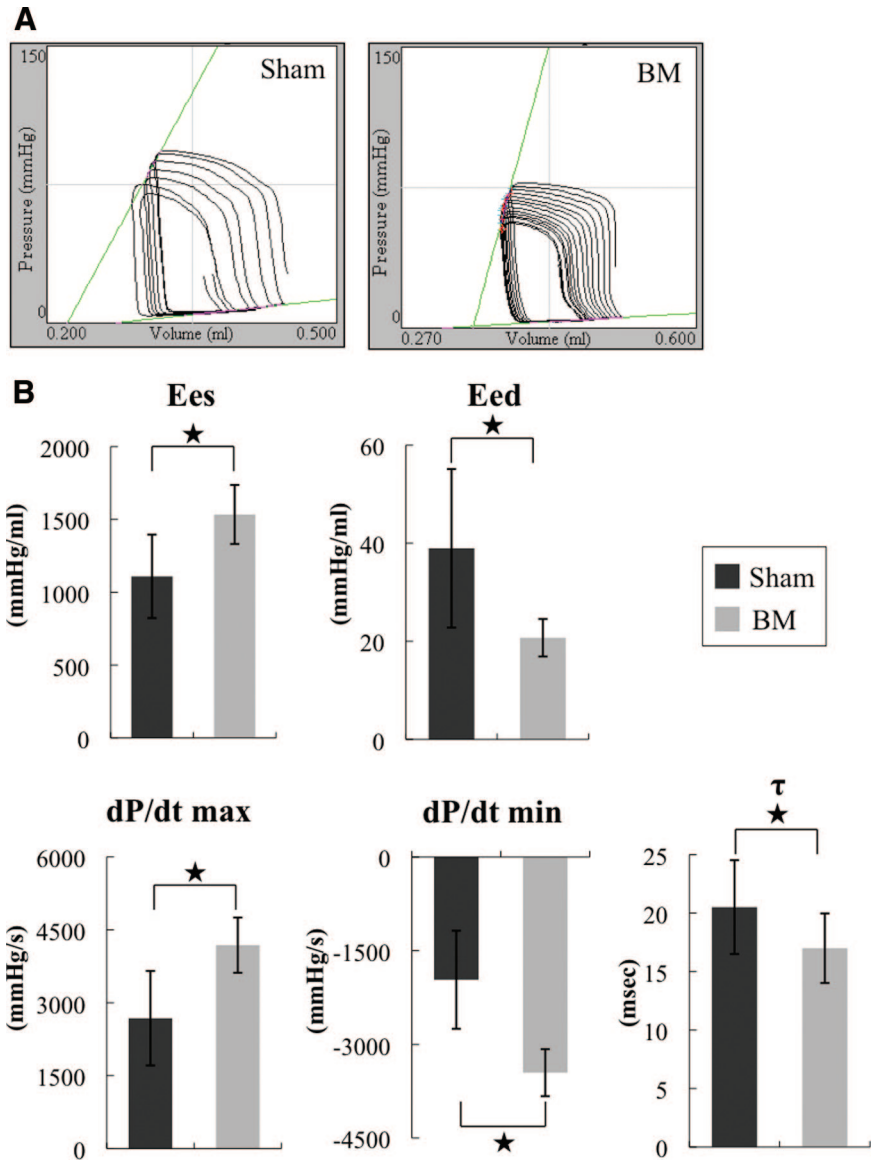

Figure 4. Effects of the induced pluripotent stem cell-derived BM on postinfarct ventricular function at 4 weeks by catheter examination. **(A):** Representative pressure-volume loops of the sham and BM groups. The systolic and diastolic performances of the BM group were significantly better than those of the sham group. **(B):** Catheter examination of Ees, Eed, dP/dt max, lower dP/dt min, and lower τ in the BM group ($n = 15$) and the sham group ($n = 15$). ★, $p < .05$. Abbreviations: BM, bioengineered myocardium; Eed, end-diastolic elastance; Ees, end-systolic elastance; max, maximum; min, minimum.

The most significant finding of the present study is the ability of the iPS cell-derived BM to improve cardiac performance, attenuate cardiac remodeling, recover wall thickness, and survive at the epicardial implantation site after implantation. These findings led us to explore the mechanism by which this improvement occurs. We believe that this improvement is achieved by two effects: (a) a direct effect of the BM synchronously contracting with the host myocardium, and (b) a paracrine effect of growth factors secreted at the site of implantation. We have previously demonstrated that (noncontracting) fibroblast sheets failed to improve systolic performance compared with neonatal cardiomyocyte sheets, and we did not observe recovery of wall thickness in the fibroblast sheet-implantation group [30]. In this study, the implanted contracting BM improved cardiac performance, recovered wall thickness, and survived at the epicardial implantation site for up to 4 weeks after implantation. This suggests that the BM, similar to neonatal cardiomyocyte sheets [30], synchronously contracts with the host myocardium and directly improves systolic performance. However, as seen in Figure 5M and 5N, DsRed-negative cells were observed in the BM on magnification images. We speculate the following explanation. In the previous study [30], we showed that host cells such as fibroblasts, endothelial cells, and some stem cells migrate into the transplanted sheet in response to HGF and VEGF. Therefore, host cells may similarly migrate into the BM. Moreover, we did not dissociate cardiomyocytes before implantation of the BM, because this destroys the extracellular matrix and gap junctions. As seen in Figure 2D, almost all of the surviving cells in no-glucose DMEM were α-actinin$^+$ cells. However, once the cardiomyocytes are dissociated, they do not reconstruct a sheet even if high-purity cardiomyocytes are seeded at a high density onto UpCell. Then, in this study, to obtain the BM as a sheet, we did

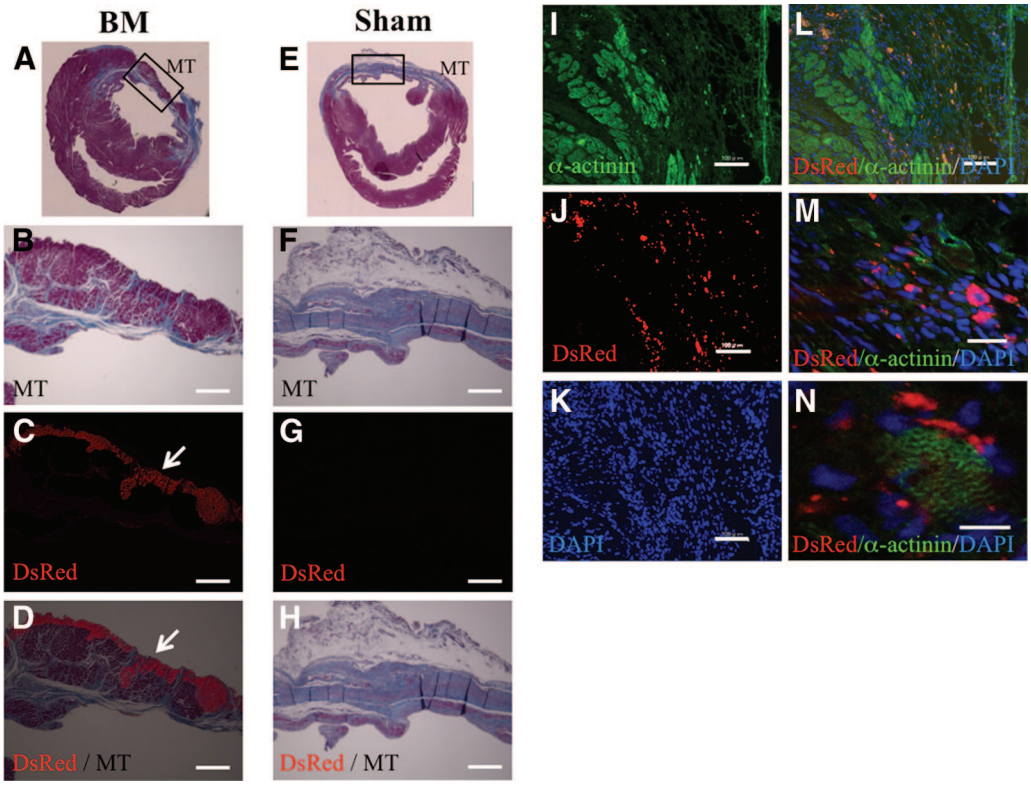

Figure 5. Histological examination of short-axis specimens at 4 weeks. **(A–H):** Microscopic images showing the whole heart and the anterior wall region in the BM group **(A–D)** and the sham group **(E–H)**. MT staining **(A, B, E, F)**. DsRed **(C, G)** was expressed in the cytosol of induced pluripotent stem (iPS) cell-derived cells in the BM group. **(D):** Merged image of **(B)** and **(C)**. **(H):** Merged image of **(F)** and **(G)**. The iPS cell-derived BM survived at the epicardial implantation site (arrows in **[C, D]**), attenuated fibrosis, and increased the thickness of the anterior wall. Scale bars = 500 μm. **(I–N):** Fluorescent microscopic images showing a part of the anterior wall region in the BM group. **(I):** Immunofluorescent histochemistry of α-actinin. DsRed was expressed in the cytosol of iPS-derived cells **(J)**; the nuclei were stained with DAPI **(K)**. **(L):** Merged image of **(I–K)**. Scale bars = 100 μm. **(M, N):** High-magnification images showing the colocalization of surviving DsRed- and α-actinin-positive cells in the anterior wall. Scale bars = 40 **(K)** and 10 μm **(L)**. Abbreviations: BM, bioengineered myocardium; DAPI, 4′,6-diamidino-2-phenylindole; DsRed, *Discosoma* red fluorescent protein; MT, Masson's trichrome.

not use a dissociation solution such as StemPro Accutase (Life Technologies, Carlsbad, CA, http://www.lifetechnologies.com) or trypsin. Therefore, α-actinin$^+$ cells were not arranged uniformly in the BM sheet, and its thickness varied throughout. For example, the section of EBs were thicker than the region of outgrowth of cells from EBs, and there were some small holes in the BM, likely representing areas of dead cells resulting from the use of no-glucose DMEM. Host cells are more likely to migrate into such areas. ELISA results revealed that elevated levels of HGF and VEGF probably contributed to the improvement of systolic performance by inducing angiogenesis and the migration of some stem cells, as observed with the implantation of skeletal myoblast sheets. Alternatively, the nondamaged host myocardium probably continues to survive after LAD coronary ligation because of the multiple autocrine or paracrine effects induced by the implanted BM, thereby improving the systolic and diastolic performances.

iPS cells can cause tumors such as teratomas; therefore, there is some apprehension regarding their use in clinical settings. We did not observe SSEA-1-positive cells by immunostaining analysis in the no-glucose DMEM-treated group. However, it is also important to acknowledge that it takes only one cell to form a tumor, and it is virtually impossible to guarantee that 100% of the cells are differentiated and safe. Therefore, to investigate the effect of no-glucose DMEM treatment on cardiomyocyte purification, we examined mice for teratomas after implantation of the BM that had been maintained for various times in no-glucose DMEM. The teratoma formation (TF) rate decreased as the period of no-glucose DMEM treatment was extended, and there was no TF in the 3-day no-glucose DMEM treatment group (supplemental online Fig. 5). Therefore, any undifferentiated cells cannot survive in no-glucose DMEM for more than 3 days.

Conclusion

We propose that the BM derived from iPS cells can improve cardiac performance and attenuate remodeling in a rat infarction model. Additional studies are required to confirm the mechanical and electrical functions in vivo; nevertheless, the BM derived from iPS cells may be a promising part of the armamentarium for the treatment of heart failure.

Acknowledgments

We thank Masako Yokoyama and Yuka Fujiwara for their excellent technical assistance. This study was partially supported by

the Japan Science and Technology Agency. K.M. is a research fellow at the Japan Society for the Promotion of Science.

Author Contributions

K.M.: conception and design, data collection, data interpretation, manuscript writing; H.U.: conception and design, data collection, data interpretation, manuscript writing assistance; A.S.: conception and design, data interpretation, manuscript revision, final approval; S.M.: conception and design, data interpretation, manuscript writing and revision, final approval; T. Sakaguchi: data interpretation; T.H.: data collection, data interpretation; T. Shimizu and T.O.: methodological assistance; S.Y.: conception and design, methodological help; Y.S.: conception and design, administrative and financial support, data interpretation, final approval.

Disclosure of Potential Conflicts of Interest

The authors indicate no potential conflicts of interest.

References

1 Lloyd-Jones D, Adams RJ, Brown TM et al. Heart disease, stroke statistics—2010 update: A report from the American Heart Association. Circulation 2010;121:e46–e215.

2 Towbin JA, Bowles NE. The failing heart. Nature 2002;415:227–233.

3 Dimmeler S, Zeiher AM, Schneider MD. Unchain my heart: The scientific foundations of cardiac repair. J Clin Invest 2005;115:572–583.

4 Murry CE, Field LJ, Menasché P. Cell-based cardiac repair: Reflections at the 10-year point. Circulation 2005;112:3174–3183.

5 Segers VF, Lee RT. Stem-cell therapy for cardiac disease. Nature 2008;451:937–942.

6 Bolli R, Chugh AR, D'Amario D et al. Cardiac stem cells in patients with ischaemic cardiomyopathy (SCIPIO): Initial results of a randomised phase 1 trial. Lancet 2011;378:1847–1857.

7 Gnecchi M, He H, Liang OD et al. Paracrine action accounts for marked protection of ischemic heart by Akt-modified mesenchymal stem cells. Nat Med 2005;11:367–368.

8 Ebelt H, Jungblut M, Zhang Y et al. Cellular cardiomyoplasty: Improvement of left ventricular function correlates with the release of cardioactive cytokines. Stem Cells 2007;25:236–244.

9 Shintani Y, Fukushima S, Varela-Carver A et al. Donor cell-type specific paracrine effects of cell transplantation for post-infarction heart failure. J Mol Cell Cardiol 2009;47:288–295.

10 Uemura R, Xu M, Ahmad N et al. Bone marrow stem cells prevent left ventricular remodeling of ischemic heart through paracrine signaling. Circ Res 2006;98:1414–1421.

11 Li X, Yu X, Lin Q et al. Bone marrow mesenchymal stem cells differentiate into functional cardiac phenotypes by cardiac microenvironment. J Mol Cell Cardiol 2007;42:295–303.

12 Reinecke H, Minami E, Zhu WZ et al. Cardiogenic differentiation, transdifferentiation of progenitor cells. Circ Res 2008;103:1058–1071.

13 Jackson KA, Majka SM, Wang H et al. Regeneration of ischemic cardiac muscle, vascular endothelium by adult stem cells. J Clin Invest 2001;107:1395–1402.

14 Nygren JM, Jovinge S, Breitbach M et al. Bone marrow-derived hematopoietic cells generate cardiomyocytes at a low frequency through cell fusion, but not transdifferentiation. Nat Med 2004;10:494–501.

15 Okano T, Yamada N, Sakai H et al. A novel recovery system for cultured cells using plasma-treated polystyrene dishes grafted with poly(*N*-isopropylacrylamide). J Biomed Mater Res 1993;27:1243–1251.

16 Shimizu T, Yamato M, Isoi Y et al. Fabrication of pulsatile cardiac tissue grafts using a novel 3-dimensional cell sheet manipulation technique, temperature-responsive cell culture surfaces. Circ Res 2002;90:e40–e48.

17 Shimizu T, Yamato M, Kikuchi A et al. Cell sheet engineering for myocardial tissue reconstruction. Biomaterials 2003;24:2309–2316.

18 Pagani FD, DerSimonian H, Zawadzka A et al. Autologous skeletal myoblasts transplanted to ischemia-damaged myocardium in humans. Histological analysis of cell survival, differentiation. J Am Coll Cardiol 2003;41:879–888.

19 Suzuki K, Murtuza B, Fukushima S et al. Targeted cell delivery into infarcted rat hearts by retrograde intracoronary infusion: Distribution, dynamics, and influence on cardiac function. Circulation 2004;110(suppl 1):II225–II230.

20 Menasché P, Hagege AA, Vilquin JT et al. Autologous skeletal myoblast transplantation for severe postinfarction left ventricular dysfunction. J Am Coll Cardiol 2003;41:1078–1083.

21 Memon IA, Sawa Y, Fukushima N et al. Repair of impaired myocardium by means of implantation of engineered autologous myoblast sheets. J Thorac Cardiovasc Surg 2005;130:1333–1341.

22 Takahashi K, Yamanaka S. Induction of pluripotent stem cells from mouse embryonic, adult fibroblast cultures by defined factors. Cell 2006;126:663–676.

23 Takahashi K, Tanabe K, Ohnuki M et al. Induction of pluripotent stem cells from adult human fibroblasts by defined factors. Cell 2007;131:861–872.

24 Yu J, Vodyanik MA, Smuga-Otto K et al. Induced pluripotent stem cell lines derived from human somatic cells. Science 2007;318:1917–1920.

25 Zhang J, Wilson GF, Soerens AG et al. Functional cardiomyocytes derived from human induced pluripotent stem cells. Circ Res 2009;104:e30–e41.

26 Zwi L, Caspi O, Arbel G et al. Cardiomyocyte differentiation of human induced pluripotent stem cells. Circulation 2009;120:1513–1523.

27 Yokoo N, Baba S, Kaichi S et al. The effects of cardioactive drugs on cardiomyocytes derived from human induced pluripotent stem cells. Biochem Biophys Res Commun 2009;387:482–488.

28 Nakagawa M, Koyanagi M, Tanabe K et al. Generation of induced pluripotent stem cells without Myc from mouse, human fibroblasts. Nat Biotechnol 2008;26:101–106.

29 Naito AT, Shiojima I, Akazawa H et al. Developmental stage-specific biphasic roles of Wnt/beta-catenin signaling in cardiomyogenesis, hematopoiesis. Proc Natl Acad Sci USA 2006;103:19812–19817.

30 Miyagawa S, Sawa Y, Sakakida S et al. Tissue cardiomyoplasty using bioengineered contractile cardiomyocyte sheets to repair damaged myocardium: Their integration with recipient myocardium. Transplantation 2005;80:1586–1595.

31 Sekiya N, Matsumiya G, Miyagawa S et al. Layered implantation of myoblast sheets attenuates adverse cardiac remodeling of the infarcted heart. Thorac J Cardiovasc Surg 2009;138:985–993.

See www.StemCellsTM.com for supporting information available online.